Expression of liver X receptor β is essential for formation of superficial cortical layers and migration of later-born neurons

Xiaotang Fan*†, Hyun-Jin Kim*, Didier Bouton*, Margaret Warner*, and Jan-Åke Gustafsson*‡

*Division of Medical Nutrition, Department of Biosciences and Nutrition, Karolinska Institutet, Novum, S-141 86 Stockholm, Sweden; and †Department of Neurobiology, Third Military Medical University, Chongqing 400038, People's Republic of China

Contributed by Jan-Åke Gustafsson, July 18, 2008 (sent for review June 26, 2008)

Liver X receptor (LXR) β regulates cholesterol levels in the brain and is essential for maintenance of motor neurons in the spinal cord and dopaminergic neurons in the substantia nigra. Here, we have examined the expression pattern of LXRβ protein in the cerebral cortex and looked for defects in cortical development in LXRβ knockout (LXR$\beta^{-/-}$) mice. LXRβ protein was widely expressed in the mouse brain at later embryonic stages, and the expression pattern in the cerebral cortex was developmentally regulated. In normal postnatal mice, LXRβ was localized mainly in the upper layers of the cerebral cortex. In LXR$\beta^{-/-}$ mice layers II and III were thinner with fewer neurons. Layer I was slightly thicker, whereas layers IV–VI were essentially normal. Consistent with this finding, Brn2 and NeuN expression were decreased in the upper layers in the LXR$\beta^{-/-}$ neonatal cortex. The number of S-phase progenitor cells in the cortex between embryonic day (E) 12.5 to E16.5, was similar in WT and LXR$\beta^{-/-}$ littermates but BrdU birth dating revealed that late-generated neurons labeled by BrdU injections administered at E14.5 or E16.5, and destined to cortical layers II/III, were disorganized and failed to migrate. The defect in migration appears to be caused by a reduction in the number of vertical processes emanating from the radial glia. These processes are the architectural guides for later-born migrating neurons. Taken together, these findings suggest that LXRβ expression in the cerebral cortex is involved in cortex lamination and is essential for the migration of late-generated neocortical neurons.

cerebral cortex | development | embryo | radial glia

The liver X receptors (LXRα and LXRβ) are members of the nuclear receptor supergene family of ligand-activated transcription factors (1, 2). LXRα and LXRβ share ≈77% amino acid sequence identity in both DNA- and ligand-binding domains and appear to bind ligands with similar affinities (3). Their endogenous ligands are oxysterols (4). LXRα and LXRβ control cholesterol metabolism and lipoprotein remodeling at both cellular and whole-body levels (5–8). Studies on LXRα and LXRβ knockout mice have revealed that LXRα plays an important role in cholesterol homeostasis, whereas LXRβ has key functions in the immune system and CNS (9–12). When both LXRs are inactivated (LXR$\alpha\beta^{-/-}$ mice), several severe abnormalities have been observed in the brain, including accumulation of lipid droplets in ependymal cells lining the ventricles, neuronal loss, and astrocyte proliferation, particularly in the substantia nigra and globus pallidus (12). In contrast, by 6 months of age, in LXR$\beta^{-/-}$ mice, there is motor dysfunction that progresses with age into hind limb paralysis (13). Part of the reason for the motor problems in these mice is activation of microglia in the substantia nigra pars reticulata and degeneration of dopaminergic neurons in the substantia nigra (14).

There is mounting evidence that many members of the nuclear receptor superfamily are essential for the precise spatial and temporal patterns of gene expression that are crucial for brain development (15). In zebrafish, the temporal expression pattern of LXR also suggests its function in the liver and CNS during development (16). In the rat and mouse, LXRβ mRNA has been reported to be widely expressed in the fetal brain (17, 18), indicating a function in brain development. However, because little information is available about the expression pattern of LXRβ protein, it remains unclear which, if any, neuronal populations are influenced by LXRβ during brain development.

In the present study, using a specific LXRβ antibody, we found that LXRβ protein was highly expressed in the mouse fetal brain at later embryonic stages. Clear developmental changes were evident in the cerebral cortex.

It is well known that mammalian cerebral corticogenesis involves layering of neurons in an "inside-out" manner, with the earliest-generated neurons positioned in the deepest layers and later-generated neurons migrating beyond previously established layers to settle at progressively more superficial levels (19–22). This inside-out gradient of migration is critical not only for cortical structure but also for establishment of correct neural connections.

Using LXR$\beta^{-/-}$ mice, we provide *in vivo* evidence that LXRβ plays important roles in the cerebral cortex development. Loss of LXRβ resulted in a smaller brain because of a reduction of the number of neurons in the superficial cortical layers. Other layers were not affected. Neuron type-specific markers confirmed this defect in the superficial layers. The reason for the defect is the inability of late-born neurons to migrate to the superficial layers, which appears to be caused by abnormalities in the vertical processes of radial glial cells along which the migrating neurons travel. Taken together, our data indicate that LXRβ protein is involved in cortex lamination and is essential for the radial migration of late-generated neocortical neurons.

Results

LXRβ Expression in Cerebral Cortex Is Developmentally Regulated. LXRβ expression appeared in the embryonic brain as early as embryonic day (E) 14.5 and at this time, some LXRβ-positive cells were specifically localized in the cortex plate (CP) (Fig. 1*A*). At E16.5, LXRβ expression in the cortex increased significantly. Most of the LXRβ-positive neurons occupied the CP, with a few positive cells in the marginal zone (MZ) and subplate (SP) (Fig. 1*B*). At E17.5 and E18.5, when late-generated neurons reach their destinations in upper layers, strong LXRβ expression was mainly in upper cortical layers, and some positive cells were observed in MZ and SP (Fig. 1*C*). On the first day of postnatal life (P0), LXRβ was localized mainly in the MZ and upper layers

Author contributions: X.F., M.W., and J.-Å.G. designed research; X.F., H.-J.K., D.B., and M.W. performed research; X.F., H.-J.K., M.W., and J.-Å.G. analyzed data; and X.F., M.W., and J.-Å.G. wrote the paper.

Conflict of interest statement: J.-Å.G. is a shareholder, grant receiver, and consultant of KaroBio AB.

‡To whom correspondence should be addressed. E-mail: jan-ake.gustafsson@mednut.ki.se.

This article contains supporting information online at www.pnas.org/cgi/content/full/0806974105/DCSupplemental.

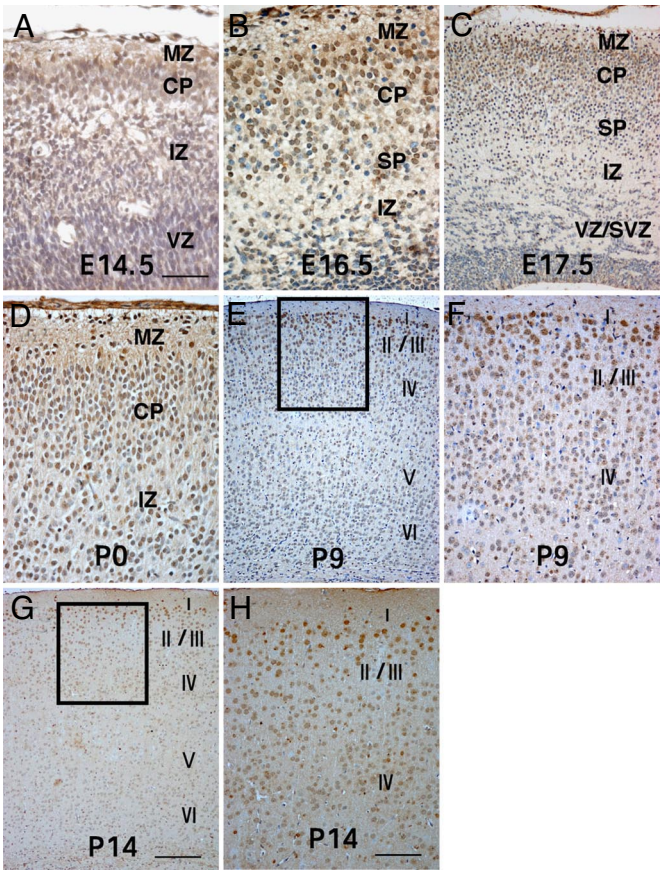

Fig. 1. LXRβ expression in the cerebral cortex. (*A*) In the E14.5 brain, only a few LXRβ-positive cells are localized in the CP. (*B*) At E16.5, LXRβ expression in brain increased significantly; most of LXRβ-positive neurons occupy the CP, with a few positive cells in MZ and SP. (*C*) By E17.5, strong LXRβ expression is seen mainly in CP, and some positive cells reside in MZ and SP. (*D*) At P0, LXRβ is localized mainly in the MZ and upper layers of the CP, a few positive cells are scattered in deep layers. (*E–H*) At P9 (*E* and *F*) and P14 (*G* and *H*) strongly LXRβ-positive neurons are localized mainly in the II/III layers, with some positive cells in the layer IV, and fewer stained cells in layers V and VI. (*F* and *H*) Higher-power views of the boxed areas in *E* and *G*. (Scale bars: *A*, *B*, and *D*, 50 μm; *C*, *F*, and *H*, 100 μm; *E* and *G*, 200 μm.)

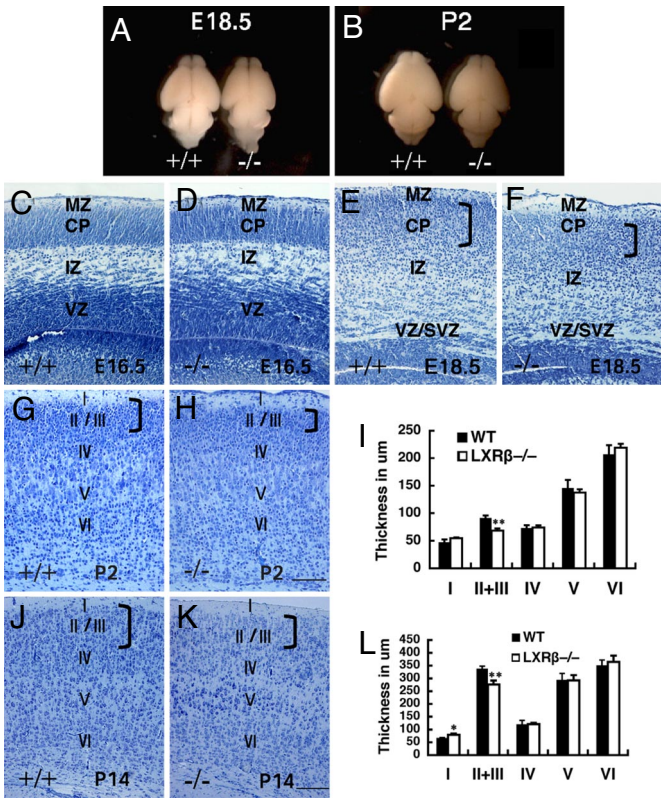

Fig. 2. Morphological alteration of the developing neocortex in the LXR$\beta^{-/-}$ mice. (*A* and *B*) Comparison between WT (+/+) and LXR$\beta^{-/-}$ brains ($^{-/-}$) of E18.5 (*A*) and P2 (*B*); the hemispheres are smaller and flatter in LXR$\beta^{-/-}$ brains ($^{-/-}$). (*C–H*, *J*, and *K*) Coronal sections of the developing cortex stained with Nissl (thionin). (*C* and *D*) There is no visible difference in the overall appearance of the cortex between WT (*C*) and LXR$\beta^{-/-}$ (*D*) mice at E16.5. (*E* and *F*) At E18.5, the CP is thinner in the LXR$\beta^{-/-}$ (*F*) mice than in WT littermates (*E*). (*G* and *H*) At P2, the upper layers seem apparently thinner with fewer neurons in LXR$\beta^{-/-}$ (*H*) mice compared with WT (G) mice, whereas layers IV through VI are essentially normal. (*K* and *J*) The thickness of II/III layers is significantly decreased in LXR$\beta^{-/-}$mice (*K*) compared with controls (*J*) at P14, whereas the thickness of layer I was lightly increased. (*I* and *L*) The thickness of cortical layers was measured at P2 (*I*) and P14 (*L*), and the results were expressed as mean $\pm$ SD. Three brains were used for each genotype. *, $P < 0.05$; **, $P < 0.01$, Student's *t* test. (Scale bars: *C–H*, 100 μm; *J* and *K*, 200 μm.)

of the CP, with a few positive cells scattered in deep layers (Fig. 1*D*). At P9, neurons strongly positive for LXRβ were more localized in the II/III layers. There were some positive cells in the layer IV and much fewer stained cells in layer V and VI (Fig. 1 *E* and *F*). At P14, neurons strongly positive for LXRβ were localized mainly in the II/III layers. Few positive cells were observed in the other layers of the cerebral cortex (Fig. 1 *G* and *H*). A few LXRβ-positive neurons were observed in the subventricular region (SVZ) and ventricular region (VZ) during embryogenesis. There was no observable LXRβ nuclear staining in the negative controls or in LXR$\beta^{-/-}$ mice. These observations indicate that mainly late-born neurons destined to superficial layers strongly express LXRβ.

Abnormality of Cerebral Cortex Development in LXRβ Mutants. Sagittal sections of E15.5 littermates revealed that brain structures, including the olfactory bulb, cerebral cortex, hippocampus, diencephalon, midbrain, pons, and medulla, were morphologically similar between LXR$\beta^{-/-}$ and WT mice. At later stages of embryogenesis and in neonates, however, differences between LXR$\beta^{-/-}$ and WT brains were readily discernible. Compared with the brains of WT mice at E18.5 and P2, the LXR$\beta^{-/-}$ mouse brains were visibly smaller (Fig. 2 *A* and *B*).

The layered structure of the cerebral cortex was examined in embryos at various stages of gestation and postnatal stages. At E14.5 and E16.5, the earlier stages examined, the histological appearance of the cerebral wall in mutants and their WT littermates was not significantly different (Fig. 2 *C* and *D*). At E18.5, however, histological differences in the neocortex were readily discernible between mutants and their WT littermates; in the mutants the CP appeared disorganized and thinner (Fig. 2 *E* and *F*). At P2 (Fig. 2 *G–I*) and P14 (Fig. 2 *J–L*), the thinning of the cerebral cortex in LXR$\beta^{-/-}$ mice was much more pronounced in layers II/III, which are formed near the end of neurogenesis (23, 24), whereas the earlier-born, deeper cortical layers were of normal to very slightly increased thickness. The MZ (layer I) was somewhat thicker in LXR$\beta^{-/-}$ mice than in WT controls at P14 (Fig. 2*L*).

Specific Reduction in Upper Cortical Layers Caused by LXRβ Deficiency. To investigate the role of LXRβ in corticogenesis, the formation of the preplate (PP) in LXR$\beta^{-/-}$ mice at E12.5 and SP in E16.5 were examined. The Tuj-1 antibody recognizes class III tubulin and is an early differentiated neuron marker (25). No gross abnormalities were detected in the expression profiles of

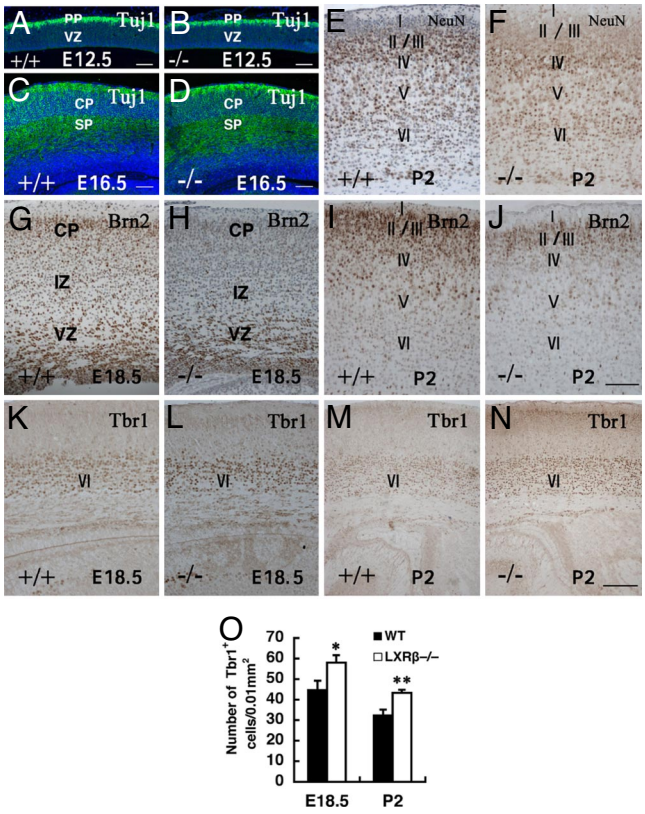

Fig. 3. Specific reduction in upper cortical layers caused by LXRβ deficiency. (*A–D*) Immunolabeling of PP and SP by Tuj-1 antibody on parasagittal sections of E12.5 (*A* and *B*) and coronal sections of E16.5 (*C* and *D*) show no difference between WT and LXR$\beta^{-/-}$ mice. (*E* and *F*) At P2, WT NeuN-stained cells are localized mostly in the II/III layers (*E*), whereas NeuN-positive cells are localized in layer IV in LXR$\beta^{-/-}$ mice (*F*). (*G–J*) Specific reduction of superficial cortical layers is also shown by decreased immunostaining of Brn2 at E18.5 (*G* and *H*) and at P2 (*I* and *J*). (*K–N*) The relatively normal deeper cortical layer thickness is demonstrated by immunostaining with Tbr1 antibody, a marker for cortical layer VI. (*O*) The density of Tbr1-positive neurons in layer VI is also shown. In the LXR$\beta^{-/-}$ mouse brain there is a significant increase in Tbr1 neuronal density ($P < 0.05$ at E18.5; $P < 0.01$ at P2 compared with WT controls, by Student's *t* test). (Scale bars: *A–D*, 100 μm; *E–L*, 100 μm; and *M* and *N*, 200 μm.)

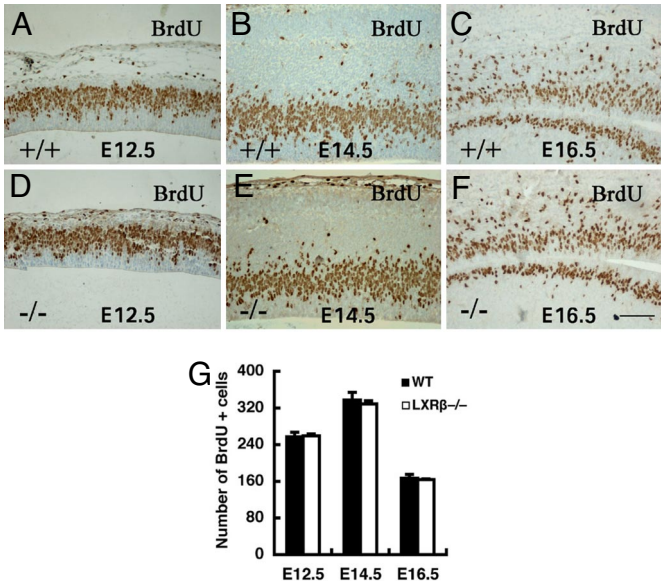

Fig. 4. Analysis of S-phase progenitor cells by BrdU pulse labeling of WT and LXR$\beta^{-/-}$ embryos at E12.5, E14.5, and E16.5. (*A–F*) A similar number of S-phase progenitor cells are in the LXR$\beta^{-/-}$ cortex relative to the WT control. (*G*) The average number of BrdU-labeled cells in the SVZ was calculated at E12.5, E14.5, and E16.5 in each field under ×40 magnification ($n = 3$; error bar, SD). There is no difference in BrdU+ cells between WT and LXR$\beta^{-/-}$. (Scale bars: *A–F*, 100 μm.)

Tuj1 between WT and LXR$\beta^{-/-}$ brains either at E12.5 (Fig. 3 *A* and *B*) or E16.5 (Fig. 3 *C* and *D*). Microtubule-associated protein 2B (MAP2B), another marker of early differentiated neurons (26), was also normal (data not shown), indicating that PP and SP formation occurs normally during early and middle corticogenesis in LXR$\beta^{-/-}$ embryos. At E18.5, NeuN-specific staining showed prominently stained upper layers in the WT brains, whereas in LXRβ mutants, more NeuN-positive neurons were localized in deep layers. At P2, clearly NeuN staining was localized mainly in layers II/III of WT controls (Fig. 3*E*), but in LXR$\beta^{-/-}$ mice more neurons were localized in layer IV, suggesting migration defects in these mice (Fig. 3*F*). The reduction in the number of neurons in the upper cortical layers was confirmed by immunostaining at E18.5 and P2 with antisera to Brn2, a marker of layers II/III and V (27) (Fig. 3 *G–J*). Moreover, the reduced Brn2-positive neural population displayed a somewhat disordered distribution in LXR$\beta^{-/-}$mice, suggesting a lamination defect. A relatively normal thickness of the deeper cortical layer at E18.5 and P2 was demonstrated by immunostaining with Tbr1, which is a marker for cortical layer VI (28). Although the thickness of layer VI appeared to be normal in the LXR$\beta^{-/-}$ mice, there was a moderate but consistent increase in the density of Tbr1 neurons (Fig. 3 *K–O*). A lamination defect specifically in layers II/III of LXR$\beta^{-/-}$mice was also confirmed by double staining with MAP2B and Brn2 [see supporting information (SI) Fig. S1].

Cortical Progenitor Cells Were Not Affected in LXR$\beta^{-/-}$ Mice. The number of cortical progenitor cells over the course of corticogenesis was detected with BrdU pulse labeling. When the embryonic brains were examined 30 min after BrdU administration, approximately equal numbers of BrdU-labeled progenitors were observed in WT and LXR$\beta^{-/-}$ mice cortices at E12.5 (Fig. 4 *A* and *D*), E14.5 (Fig. 4 *B* and *E*), and E16.5 (Fig. 4 *C* and *F*), suggesting that a similar number of progenitor cells are produced in WT and LXR$\beta^{-/-}$ mice during the course of corticogenesis.

LXRβ Is Important for Later-Born Neuron Migration. BrdU birth dating was used to examine whether the abnormalities in cortical layering reflected abnormal neuronal migration. When analyzed at E18.5, neurons labeled at E14.5 in the WT cortex resided in the CP (Fig. 5 *A* and *C*). In LXR$\beta^{-/-}$ mice BrdU-positive neurons were disorganized and less numerous in the CP, with more labeled cells remaining in the intermediate zone (IZ) (Fig. 5 *B* and *D*). When BrdU was administered at E16.5, there were fewer cells labeled in the CP in mutants compared with WT littermates (Fig. 5 *F* and *G*). When analyzed in the WT cortex at P14, neurons labeled at E14.5 were in layers II/III and layer IV, with fewer cells in the layer V and VI (Fig. 5 *H* and *J*). In contrast, in LXR$\beta^{-/-}$ mice, neurons born at E14.5 were still localized mainly in the deep layers (V and VI) by day P14. There were few cells in layers II/III (Fig. 5 *I* and *K*). When BrdU was administered at E16.5 there were fewer BrdU-labeled cells in the layers II/III in LXR$\beta^{-/-}$ mice than in WT littermates (Fig. 5 *M* and *N*), suggesting that the neurons that are mispositioned are nevertheless able to migrate and reach the appropriate target layers II/III. These data, along with the NeuN and Brn2 immunostaining, suggest that LXRβ deficiency results in a defect in radial migration in later-born neurons.

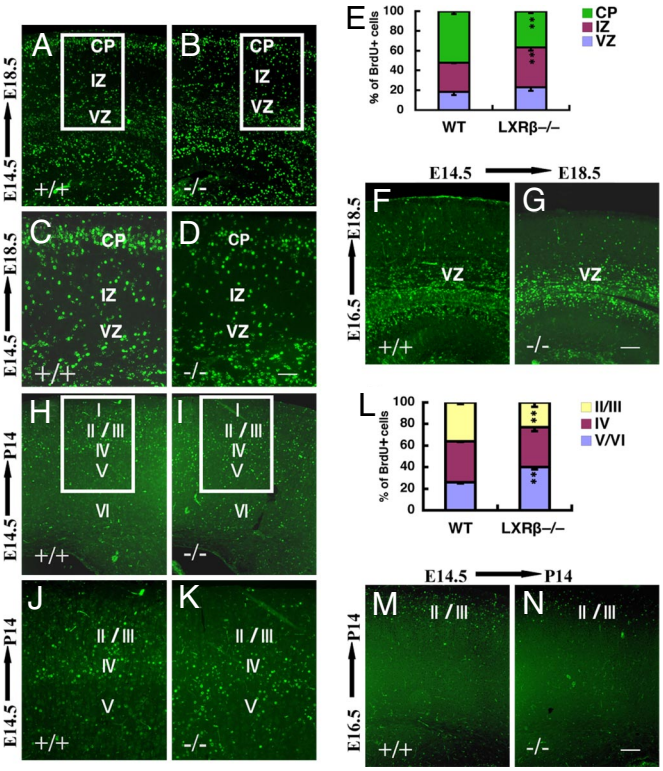

Fig. 5. Defect in later-born neuronal migration of LXR$\beta^{-/-}$ cortex. (*A–D*) Neurons labeled at E14.5 and analyzed at E18.5 accumulated in the VZ/SVZ and IZ. There are fewer labeled cells in the CP of LXR$\beta^{-/-}$ mouse embryos (*B* and *D*) compared with WT littermates (*A* and *C*). *C* and *D* are higher-power views of the boxed areas in *A* and *B*. (*E*) The histogram shows the distribution of BrdU+ cells at E18.5 when labeled at E14.5 and analyzed in the different compartments of the cortex (VZ/SVZ, IZ, and CP) as a way to quantify radial migration in the different genotypes. Asterisks indicate significant differences in percentages of BrdU-positive cells in a given cortical zone in mutant and WT cortices ($n = 3$; **, $P < 0.01$). (*F* and *G*) Neurons labeled at E16.5 and analyzed at E18.5 were located mostly in the SVZ and IZ of LXR$\beta^{-/-}$ mutant embryos (*G*) but in WT embryos (*F*) the labeled neurons had migrated to the outer layers. (*H* and *J*) When neurons were labeled at E14.5 and analyzed at P14, there were more labeled cells in layers II/III and layer IV and fewer cells in layer V and VI in the WT mouse brains. (*I* and *K*) The pattern of BrdU labeled cells is inverted in the mutant cortex, with positive cells localized mainly in the deep layers (V and VI) and with few cells in layers II/III. *J* and *K* are higher-power views of the boxed areas in *H* and *I*. (*L*) The histogram shows the distribution at P14 of BrdU-positive cells (labeled at E14.5) in the different compartments of the cortex (II/III, IV, and V/VI). Asterisks indicate significant differences in percentages of BrdU-positive cells in a given cortical zone in mutant and WT cortices ($n = 3$; **, $P < 0.01$). (*M* and *N*) When BrdU was administered at E16.5, and analyzed at P14, there were fewer BrdU-labeled cells in layers II/III of LXR$\beta^{-/-}$ mice (*N*) compared with WT littermates (*M*). (Scale bars: *A*, *B*, *F*, *G*, *J*, and *K*, 100 μm; *C* and *D*, 50 μm; *H*, *I*, *M*, and *N*, 200 μm.)

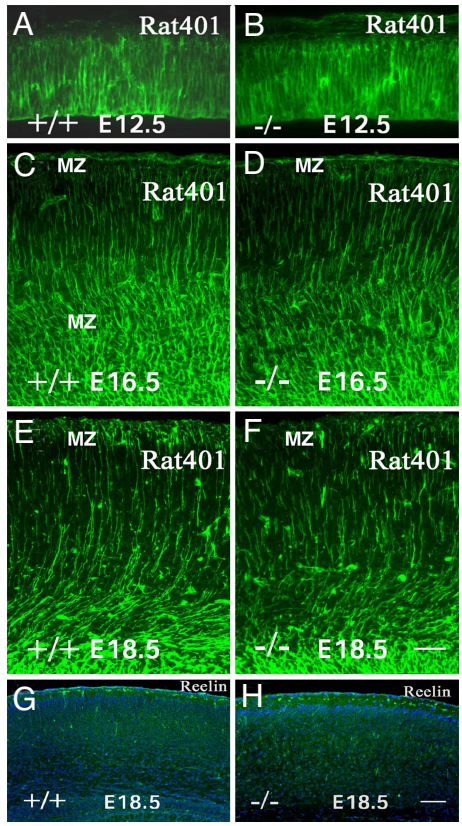

Fig. 6. Abnormalities in radial glia and normal reelin expression in LXR$\beta^{-/-}$ mutants. (*A–F*) Nestin staining of E12.5, E16.5, and E18.5 cortices. (*A* and *B*) The pattern and distribution of radial glial fibers is comparable in WT (*A*) and LXR$\beta^{-/-}$ (*B*) mice at E12.5. (*C* and *D*) At E16.5, In WT controls there are many radially distributed processes extending throughout the full thickness of the CP (*C*), whereas, in LXR$\beta^{-/-}$ mice, some nestin-stained fibers fail to extend through the full thickness of the cerebral wall (*D*). (*E* and *F*) At E18.5, disruption of radial fibers is apparent in mutant cortices (*F*) compared with WT (*E*). (*G* and *H*) In contrast, reelin expression (green) is comparable in WT (*G*) and LXR$\beta^{-/-}$ (*H*) mice at E18.5. Nuclei were counterstained with DAPI (blue). (Scale bars: *A–F*, 50 μm; *G* and *H*, 100 μm.)

The Radial Glial Scaffold Was Altered in LXR$\beta^{-/-}$ Mice. Correct neuronal migration requires radial glial fibers and Cajal-Retzius cells (29–31). At E12.5, nestin immunostaining of the cortex of LXR$\beta^{-/-}$ embryos (Fig. 6*B*) appeared similar to that in WT embryos (Fig. 6*A*), with many radially distributed processes extending throughout the telencephalic wall. At E16.5, nestin staining in WT controls continued to show many radially distributed processes extending throughout the full thickness of the cerebral hemispheres (Fig. 6*C*). In contrast, at E16.5, in LXR$\beta^{-/-}$ mice, nestin staining fibers failed to extend through the full thickness of the cerebral wall (Fig. 6*D*). At E18.5, in WT mice, substantial numbers of radial glial cell processes were seen extending from the ventricular surface to layer I, where they branched into several endfeet and were organized into a well defined layer (Fig. 6*E*). In mutant mice, the number of vertical processes extending through the full thickness of the cerebral cortex and endfeet in layer I were decreased (Fig. 6*F*). Neither the number of Cajal–Retzius neurons nor the intensity of their immunostaining for Reelin was affected by the loss of LXRβ (Fig. 6 *G* and *H*). These data suggest that a disrupted radial glial fiber system contributes to the abnormal radial migration of neurons in LXR$\beta^{-/-}$ mice.

Nestin is regulated in a cell-cycle-dependent manner during neurogenesis, and Brn2 is a transcription factor essential for the down-regulation of nestin (32). If nestin filaments do not depolymerize during proliferation, the radial glial processes will fragment. The lower level of Brn2 and the disorganization in the cerebral cortex observed in LXR$\beta^{-/-}$ mice may indicate an abnormal regulation of nestin gene expression.

Discussion

In the present study, we demonstrate that LXRβ expression first appears in the cerebral cortex as early as E14.5. At this age there were a few weakly stained cells localized in the CP. At the end of gestation, LXRβ was strongly expressed in the CP from E16.5 until E18.5. After birth, LXRβ was localized mainly in layers II/III. The pattern of LXRβ protein expression in the CP indicates that LXRβ could affect development of CP, which

prompted us to investigate how LXRβ might influence cortical development.

At early embryonic stages, LXR$\beta^{-/-}$ brains appeared relatively normal; however, defects in LXR$\beta^{-/-}$ brains were readily discernible at later stages of embryogenesis and in the neonatal period. Furthermore, no gross abnormalities in the generation of neurons were detected by either Tuj1 or MAP2B antibodies at E12.5 or E16.5. The finding that early corticogenesis was not notably affected in LXR$\beta^{-/-}$ brains is in good accordance with the fact that LXRβ was expressed in the CP at later embryonic stages. Nissl staining showed that the CP was thinner in the LXR$\beta^{-/-}$ mice at E18.5. At P2 and P14, it is apparent that layers II/III, in particular, are diminished in thickness. Neurons in layers V and VI, which are born at an early embryonic stage and express LXRβ at lower levels, appeared to be normal in the LXR$\beta^{-/-}$ mice. Thus LXRβ is essential for development of upper layers, and the formation of deep layers is largely independent of LXRβ signaling. This conclusion is supported by our observation that the layer marked by Brn2 antibody, which normally marks a population of neurons in layers II/III, is substantially narrower and disorganized in LXR$\beta^{-/-}$ mice compared with WT mice. The CP grows in an inside-out order, from the innermost layer VI comprising the earliest-born cortical neurons to the outer layer II containing the latest-born neurons (19, 20). As the cortical neurons are derived from the neocortical ventricular proliferative zone, neurogenesis (between E12 and E17 in mouse) in the cortical ventricular zone progenitors requires a precise timing of cell division (33, 34). We further demonstrated that approximately equal numbers of BrdU-labeled progenitors were observed in WT and LXR$\beta^{-/-}$ mouse cortices between E12.5 and E16.5, suggesting that cortical defects in LXR$\beta^{-/-}$ brains are not caused by the production of progenitor cells during the course of corticogenesis. In support of this idea, Tbr1 staining was normal between E12.5 and E16.5 in LXR$\beta^{-/-}$ brains.

Between E18.5 and P2, prominently NeuN stained neurons were found in the upper layers of WT brains, whereas in LXRβ mutants more strongly stained neurons localized in deep layers. This finding indicates that loss of LXRβ may cause a migration defect in later differentiated neurons. In LXR$\beta^{-/-}$ mice, BrdU birth-dating experiments revealed that migration of later-born neurons (exposed to BrdU at E14.5 and E16.5) to upper layers was retarded, because more labeled cells were found in deep layers. These results suggest that radial migration was altered in LXR$\beta^{-/-}$ mice.

It is well known that the cells destined to layers V and VI are early-generated neurons that start to migrate before E14.5, likely using somal translocation to move from the germinal ventricular zone to their definitive positions in the CP. Somal translocation involves movement of neurons toward the surface of the brain independent of radial glial guidance, which occurs through attachment of the neuron's own radial leading process to the surface of the brain and translocation of the cell body upon shortening of the process (35). This mode of migration may be necessary in the absence of a glial scaffold early in the development of the cortex. By contrast, later-generated neurons destined to superficial cortical layers follow thereafter and may increasingly use radial glia-guided migration (35–37). As these late-forming layers are affected in the LXR$\beta^{-/-}$ mutant, this fact suggests that late glia-guided migration is controlled by LXRβ signaling, which is consistent with the finding that in the WT cortex the strongest LXRβ expression was found in upper cortical layers.

After staining for nestin, an intermediate filament shared by radial glial cells and neuronal precursors (38), the processes of the radial glial cells in LXR$\beta^{-/-}$ mice appeared to be truncated or less organized into radial formations. Such abnormal processes might not be able to provide guidance for migrating neurons. One recent study (32) has demonstrated that nestin is regulated in a cell-cycle-dependent manner during the neurogenesis and Brn2 is a transcription factor essential for the down-regulation of nestin. In combination with Brn2 staining in the cerebral cortex of LXR$\beta^{-/-}$ mice, this finding indicates that Brn2 may partly contribute to abnormal regulation of nestin gene expression and then affect fragmentation of glial processes. Cajal-Retzius cells, which secrete reelin, are directly involved in the regulation of the radial glial phenotype, and reeler mutants display a reduction in the extension of radial fibers (39). The number of Cajal-Retzius neurons and the intensity of their staining for reelin were not altered in the LXR$\beta^{-/-}$ mouse cortex, suggesting that the defect in radial glial cells in LXR$\beta^{-/-}$ mice was independent of reelin level. Apparently, a disrupted radial glial fiber system contributes to the abnormal radial migration of neurons in LXR$\beta^{-/-}$ mice.

The cortical abnormalities described here for LXR$\beta^{-/-}$ mice are reminiscent of the defects produced by apolipoprotein E (ApoE) receptor 2 (ApoER2) mutations in mouse in affecting cortical lamination. Because ApoE is an LXR-regulated gene, the role of defects in ApoE signaling in the LXR$\beta^{-/-}$ mice has to be considered. In the ApoER2 mutant mice, early-generated layers are formed almost normally, but the formation of superficial, late-generated layers is severely altered. Late-born cells are unable to bypass earlier ones and remain close to the ventricular zone (40). ApoE is not the only possible pathway through which LXR may regulate neuronal migration. Recently, cross-talk between TGF-β and LXR-signaling pathways has been demonstrated (41). TGF-β and LXR agonists have synergistic effects on LXR target genes in mouse embryonic fibroblasts. Both pathways involve the intracellular mediator Smad3 and share a common coactivator protein, RAP250 (41). Interestingly, *in vitro* studies have demonstrated that TGF-β1 might be a novel factor involved in radial glial development and in the integrity of radial glial processes (42).

In the present study, another function of LXRβ in the CNS has been uncovered. We have shown that LXRβ plays an important role in brain development and is essential for cortex lamination and migration of later-born neurons through modulation of radial glial cells. It is likely that LXRβ modulates radial glial cells through modulating ApoE or TGF-β signaling.

Materials and Methods

Animals and Tissue Preparation. The generation of LXR$\beta^{-/-}$ mice has been described (9). Heterozygous mice were used for breeding. The day of vaginal plug detection was designated as E0.5. To obtain embryos, pregnant mice were anesthetized deeply with CO_2 and perfused with PBS followed by 4% paraformaldehyde (in 0.1 M PBS, pH 7.4). Embryos were taken out and put on ice, and brains were dissected and postfixed in the same fixative overnight at 4°C. For the P2 pups and P14 young mice, brains were dissected and postfixed in 4% paraformaldehyde overnight at 4°C. Tails and limbs were removed for genotyping. After fixation, brains were processed for paraffin (5 μm) sections.

Preparation of Antibodies to LXRβ. The goat polyclonal LXRβ antibody is directed against the N-terminal region of mouse LXRβ, amino acids 1–17. IgG was purified by polyethylene glycol precipitation and chromatography on Wharman DE52 cellulose. Preabsorbed antibodies were prepared by incubating LXRβ antibodies for 12 h at 4°C with LXRβ protein coupled to activated Sepharose.

Immunohistochemistry. In this study we used Nissl staining to examine the histology of brains with light microscopy. Paraffin sections were deparaffinized in xylene, rehydrated through graded alcohol, and processed for antigen retrieval by boiling in 10 mM citrate buffer (pH 6.0) for 2 min. The sections were incubated in 0.5% H_2O_2 in PBS for 30 min at room temperature to quench endogenous peroxidase and then incubated in 0.5% Triton X-100 in PBS for 30 min. To block nonspecific binding, sections were incubated in 3% BSA for 1 h at 4°C. For LXRβ staining, retrieval was improved by incubating the sections with 0.15 units/ml of β-galactosidase for 2 h. Sections were then incubated with anti-LXRβ (1:200), anti-Tbr1 (1:200), anti-NeuN (1:500), anti-

Tuj1 (1:1,000), anti-Brn2 (1:200), anti-Rat401 (which recognizes nestin) (1:50), anti-reelin (1:200), anti-calretinin (1:1,000), or anti -MAP2B (1:200) in 1% BSA and 0.1% Triton 100 overnight at room temperature. BSA replaced primary antibodies in negative controls. After washing, sections were incubated with the corresponding secondary antibodies in 1:200 dilutions for 2 h at room temperature, followed by the avidin-biotin-peroxidase complex for 2 h and 3,3-diaminobenzidine tetrahydrochloide as the chromagen.

BrdU Labeling and Analysis. Pregnant females were injected i.p. with 50 mg/kg BrdU in 0.9% NaCl with 0.007 M NaOH. For analysis of S-phase progenitor cells, BrdU was given in single i.p. injections at E12.5, E14.5, and E16.5. Embryos were removed 30 min later. For the birth-dating study, BrdU was given in single i.p. injections at E14.5 or E16.5, embryos were removed at E18.5, four pregnant females were left to give birth, and their offspring were analyzed 2 weeks postnatally. The paraffin-embedded brain sections were dewaxed in xylene, rehydrated, processed for antigen retrieval with 10 mM citrate buffer (pH 6.0), and then incubated in 2 M HCl for 10 min at room temperature. This procedure was followed by neutralization in 0.05 M borate buffer (pH 8.5) for 15 min and blocking of endogenous peroxidase with 1% H_2O_2 for 30 min. Sections were then immunostained with an anti-BrdU mAb (1:100) overnight at 4°C followed by biotinylated goat anti-mouse secondary antibody (1:200) and avidin-biotin peroxidase complex (1:200) for 2 h at room temperature. After sections were washed in PBS, BrdU immunostaining was revealed by using 3,3-diaminobenzidine peroxidase. For progenitor cell counting, the number of BrdU+ cells in the SVZ was calculated at E12.5, E14.5, and E16.5 in each field under ×40 magnification. For radial migration analysis, the distribution of BrdU-positive cells was analyzed in the different compartments of the cortex (VZ/SVZ, IZ, and CP at E18.5 and II/III, IV, and V/VI at P14), the percentage of BrdU-labeled cells in each area was determined, and results were plotted as histograms.

Data Analysis. Quantitative measurement of cortical thickness was performed on photomicrographs of comparable coronal sections for each genotype by using image processing and analysis software. The number of mice in each experiment was at least three per genotype. Data are presented as mean ± SD. The statistical significance of differences between LXR$\beta^{-/-}$ and control samples was assessed by using Student's *t* test.

Chemicals and Antibodies. We purchased β-galactosidase from Sigma–Aldrich. The following antibodies were used: rabbit anti-calretinin (zcomSwant), mouse anti-BrdU (BD Pharmingen), mouse anti-Tuj1 (Promega), mouse anti-MAP2B (BD Transduction), rabbit anti-Tbr1 (Abcam, rabbit polyclonal anti-Brn2 (Santa Cruz Biotechnology), mouse anti-Rat401 (Development Studies Hybridoma Bank, and mouse anti-NeuN and anti-reelin (Chemicon). The goat polyclonal anti-LXRβ was produced in our laboratory at the Karolinska Institutet , FITC anti-mouse antibody was from Jackson ImmunoResearch, and biotinylated goat anti-rabbit IgG, rabbit anti-goat IgG, and goat anti-mouse IgG were from Zymed.

ACKNOWLEDGMENTS. This study was supported by the Swedish Science Council, KaroBio AB, and the European Union Integrated Project CRESCENDO.

1. Teboul M, *et al.* (1995) OR-1, a member of the nuclear receptor superfamily that interacts with the 9-cis-retinoic acid receptor. *Proc Natl Acad Sci USA* 92:2096–2100.
2. Apfel R, *et al.* (1994) A novel orphan receptor specific for a subset of thyroid hormone-responsive elements and its interaction with the retinoid/thyroid hormone receptor subfamily. *Mol Cell Biol* 14:7025–7035.
3. Alberti S, Steffensen KR, Gustafsson JA (2000) Structural characterization of the mouse nuclear oxysterol receptor genes LXRα and LXRβ. *Gene* 243:93–103.
4. Janowski BA, *et al.* (1999) Structural requirements of ligands for the oxysterol liver X receptors LXRα and LXRβ. *Proc Natl Acad Sci USA* 96:266–271.
5. Tontonoz P, Mangelsdorf DJ (2003) Liver X receptor signaling pathways in cardiovascular disease. *Mol Endocrinol* 17:985–993.
6. Zelcer N, Tontonoz P (2006) Liver X receptors as integrators of metabolic and inflammatory signaling. *J Clin Invest* 116:607–614.
7. Janowski BA, Willy PJ, Devi TR, Falck JR, Mangelsdorf DJ (1996) An oxysterol signalling pathway mediated by the nuclear receptor LXRα. *Nature* 383:728–731.
8. Repa JJ, Mangelsdorf DJ (2000) The role of orphan nuclear receptors in the regulation of cholesterol homeostasis. *Annu Rev Cell Dev Biol* 16:459–481.
9. Alberti S, *et al.* (2001) Hepatic cholesterol metabolism and resistance to dietary cholesterol in LXRβ-deficient mice. *J Clin Invest* 107:565–573.
10. Robertson KM, *et al.* (2005) The liver X receptor β is essential for maintaining cholesterol homeostasis in the testis. *Endocrinology* 146:2519–2530.
11. Steffensen KR, *et al.* (2004) Genome wide expression profiling: A panel of mouse tissues discloses novel biological functions of liver X receptors in adrenals. *J Mol Endocrinol* 33:609–622.
12. Wang L, *et al.* (2002) Liver X receptors in the central nervous system: From lipid homeostasis to neuronal degeneration. *Proc Natl Acad Sci USA* 99:13878–13883.
13. Andersson S, Gustafsson N, Warner M, Gustafsson JA (2005) Inactivation of liver X receptor β leads to adult-onset motor neuron degeneration in male mice. *Proc Natl Acad Sci USA* 102:3857–3862.
14. Kim HJ, *et al.* (2008) Liver X receptor β (LXRβ): A link between β-sitosterol and amyotrophic lateral sclerosis-Parkinson's dementia. *Proc Natl Acad Sci USA* 105:2094–2099.
15. Gofflot F, *et al.* (2007) Systematic gene expression mapping clusters nuclear receptors according to their function in the brain. *Cell* 131:405–418.
16. Archer A, Lauter G, Hauptmann G, Mode A, Gustafsson JA (2008) Transcriptional activity and developmental expression of liver X receptor (lxr) in zebrafish. *Dev Dyn* 237:1090–1098.
17. Kainu T, Kononen J, Enmark E, Gustafsson JA, Pelto-Huikko M (1996) Localization and ontogeny of the orphan receptor OR-1 in the rat brain. *J Mol Neurosci* 7:29–39.
18. Annicotte JS, Schoonjans K, Auwerx J (2004) Expression of the liver X receptor α and β in embryonic and adult mice. *Anat Rec A Discov Mol Cell Evol Biol* 277:312–316.
19. Angevine JB, Sidman RL (1961) Autoradiographic study of cell migration during histogenesis of cerebral cortex in the mouse. *Nature* 192:766–768.
20. Rakic P (1974) Neurons in rhesus monkey visual cortex: Systematic relation between time and origin and eventual disposition. *Science* 183:425–427.
21. Rakic P (1988) Specification of cerebral cortical areas. *Science* 241:170–176.
22. Hatten ME (1993) The role of migration in central nervous system neuronal development. *Curr Opin Neurobiol* 3:38–44.
23. Caviness VS, Jr (1982) Neocortical histogenesis in normal and reeler mice: A developmental study based upon [^{3}H]thymidine autoradiography. *Brain Res* 256:293–302.
24. Smart IH, Smart M (1982) Growth patterns in the lateral wall of the mouse telencephalon: I. Autoradiographic studies of the histogenesis of the isocortex and adjacent areas. *J Anat* 134:273–298.
25. Geisert, EE, Jr, Frankfurter A (1989) The neuronal response to injury as visualized by immunostaining of class III-tubulin in the rat. *Neurosci Lett* 102:137–141.
26. Crandall JE, Jacobson M, Kosik KS (1986) Ontogenesis of microtubule-associated protein 2 (MAP2) in embryonic mouse cortex. *Brain Res* 393:127–133.
27. McEvilly RJ, de Diaz MO, Schonemann MD, Hooshmand F, Rosenfeld MG (2002) Transcriptional regulation of cortical neuron migration by POU domain factors. *Science* 295:1528–1532.
28. Hevner RF, *et al.* (2001) Tbr1 regulates differentiation of the preplate and layer 6. *Neuron* 29:353–366.
29. Feng L, Hatten ME, Heintz N (1994) Brain lipid-binding protein (BLBP): A novel signaling system in the developing mammalian CNS. *Neuron* 12:895–908.
30. Lois C, Garcia-Verdugo JM, Alvarez-Buylla A (1996) Chain migration of neuronal precursors. *Science* 271:978–981.
31. Soriano E, Del Rio JA (2005) The cells of cajal-retzius: Still a mystery one century after. *Neuron* 46:389–394.
32. Sunabori T, *et al.* (2008) Cell-cycle-specific nestin expression coordinates with morphological changes in embryonic cortical neural progenitors. *J Cell Sci* 121:1204–1212.
33. Caviness VS, Jr, Takahashi T, Nowakowski RS (1995) Numbers, time, and neocortical neuronogenesis: A general developmental and evolutionary model. *Trends Neurosci* 18 : 379–383.
34. Takahashi T, Nowakowski RS, Caviness, VS, Jr (1995) The cell cycle of the pseudostratified ventricular epithelium of the embryonic murine cerebral wall. *J Neurosci* 15:6046–6057.
35. Nadarajah B, Parnavelas JG (2002) Modes of neuronal migration in the developing cerebral cortex. *Nat Rev Neurosci* 3:423–432.
36. Sanada K, Gupta A, Tsai LH (2004) Disabled-1-regulated adhesion of migrating neurons to radial glial fiber contributes to neuronal positioning during early corticogenesis. *Neuron* 42:197–211.
37. Kriegstein AR, Gotz M (2003) Radial glia diversity: A matter of cell fate. *Glia* 43:37–43.
38. Frederiksen K, McKay RD (1988) Proliferation and differentiation of rat neuroepithelial precursor cells *in vivo*. *J Neurosci* 8:1144–1151.
39. Hartfuss E, *et al.* (2003) Reelin signaling directly affects radial glia morphology and biochemical maturation. *Development* 130: 4597–4609.
40. Hack I, *et al.* (2007) Divergent roles of ApoER2 and Vldlr in the migration of cortical neurons. *Development* 134:3883–3891.
41. Antonson P, *et al.* (2008) RAP250 is a coactivator in the transforming growth factor β signaling pathway that interacts with Smad2 and Smad3. *J Biol Chem* 283:8995–9001.
42. Stipursky J, Gomes FC (2007) TGF-β1/SMAD signaling induces astrocyte fate commitment *in vitro*: Implications for radial glia development. *Glia* 55:1023–1033.